Increases in Hot Pixel Development Rates for Small Digital Pixel Sizes

Glenn H. Chapman, Rahul Thomas, Rohan Thomas, Klinsmann J. Coelho Silva Meneses, Tommy Q. Yang; School of Engineering Science Simon Fraser University, Burnaby, B.C., Canada, V5A 1S6 glennc@ensc.sfu.ca, rmt3@sfu.ca, rohant@sfu.ca, klinsmannjoel@hotmail.com, tqyang@sfu.ca

Israel Koren, Zahava Koren; Dept. of Electrical and Computer Engineering, University of Massachusetts, Amherst, MA, 01003 koren,zkoren@ecs.umass.edu

Abstract

The rising demand for digital imagers has resulted in the push to reduce pixel size while increasing imager sensitivity, which in turn, results in an increasing rate of defects that develop in the field. Research has shown that "Hot Pixels" are the most common type of defects in modern digital imagers, with their number in a given imager increasing over time. In our previous studies we had developed an empirical formula to project the growth rate of hot pixel defects in terms of defects/year/mm². We discovered that hot pixel densities tend to grow via a power law of the inverse of the pixel size raised to the power of about 3. This paper explores the effects on defect growth rate, of reducing pixel sizes even more, specifically in cell phone imagers. Due to lack of noise suppression algorithms in these imagers, we have developed specialized procedures for analyzing the collected dark frame data. We also ensure that hot pixel detections in cell phone cameras are statistically significant within the error margins. Our current results confirm the accelerated growth rate for this small pixel range, emphasizing the need for caution by designers and further study in this area of defect development.

Keywords- imager defect detection, hot pixel development, APS/CCD defects rates, active pixel sensor APS, CCD, cellphone imagers

Introduction

The field of digital imaging and its associated technology has become a central theme in today's world of photography. Digital imagers have spread into everyday devices, ranging from consumer products, such as cell phones, to cars via embedded sensors. Their role in medical, industrial, and scientific applications is becoming more and more vital in many engineering solutions. The inherent result is a drive to enhance these sensors via a decrease in pixel size and an increase in the sensitivity of the imager. As with other microelectronic devices, digital imagers develop defects over time, and the nature of the sensor makes it more sensitive to defects that most likely would not affect other devices. In contrast to other devices, in-field defects in digital imagers begin to manifest themselves soon after fabrication. These defects are permanent and continuously increase in number over the sensor's lifetime, eventually degrading image quality. This is a serious problem for various applications where image quality/pixel sensitivity is important.

Research has shown [1-6] that "Hot Pixels" are the most common type of defects in modern digital imagers, with their number in a given sensor increasing over time. Previous work has shown they are likely caused by cosmic rays [1-3], hence shielding or fabrication changes cannot fully prevent their manifestation and the increase in their number with time. Hot pixels have an offset value plus a coefficient of growth with exposure time, both of which increase with the sensitivity

but remain constant after formation. In our previous studies we have developed an empirical formula relating the defect density D (defects per year per mm² of sensor area) to the pixel size S (in microns) and sensor gain (ISO). We discovered that hot pixel densities grow via a power law of the inverse of the pixel size raised to a power of about 3.

It is important to understand how the decrease in pixel size affects the hot pixel growth rate. The hot pixel growth equations were obtained based on data from DSLR cameras in the higher range of pixel sizes (6 - 7 µm) and point-and-shoot cameras in the midrange pixel sizes (3 - 4 µm). In the small pixel size range (2 - 3 µm), multiple cell phone cameras of the same model were used. However, for the smaller pixel sizes, the point and shoot and cell phone data could previously be taken only with jpg images, for which hot pixel detection is less accurate. This paper explores the effects of smaller pixel sizes on hot pixel manifestation to provide better estimates in the 3 to 1 µm range. Current DSLRs use 3 - 4 µm in the midrange enabling us to acquire RAW images at these smaller pixel sizes with higher accuracy over a wider range of ISOs, thus providing a more accurate data to create updated growth models. These parameters are obtained for each hot pixel by using a dark frame exposure with increasing exposure times. Obtaining this data for each camera involves typically 5 to 20 calibration images per test at a wide range of exposure times and ISOs, and their analysis with specialized software.

The organization of this paper is as follows: We first present the classical model of imager *hot pixels*. We then describe the growth rate of hot pixels. The next section discusses expanded research with imagers that contain smaller pixel sizes. We next present a defect analysis for modern cell phone cameras, and later discuss results with smaller pixel sizes. Finally, we present the paper's conclusions.

Hot Pixels

Over the past 11 years [5,6], we have been studying the characteristics of imager defects by manually calibrating many commercial cameras, including 29 DSLRs (Digital Single Lens Reflex cameras). We exposed them to a dark frame (i.e., no illumination) at increasing exposure times, and recorded any brightness in the resulting images. This experimental strategy helped us to identify different types of hot pixels (stuck-high vs. partially stuck defects). Until now, however, we have not identified any stuck-high hot pixels in our data. Figure 1 displays the different pixel responses possible in a dark frame, where level 0 represents no illumination and level 1 represents saturation. Three different pixel responses are shown in Figure 1. Firstly, a good pixel behavior is displayed as curve (a). Since there is no illumination, we expect the pixel output to be constantly zero for all exposure times. The other two curves depict the two different types of hot pixels [5]. Curve (b) is a standard hot pixel, which has an illumination-independent component that increases linearly with exposure time. The third response shown as curve (c) is a partially stuck hot pixel, which has an additional offset that manifests itself even at no exposure.
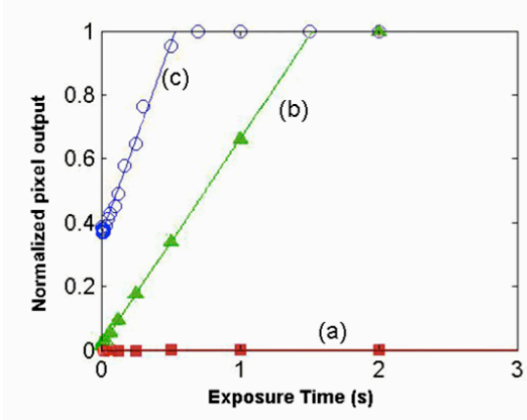
Figure 1: Comparing the dark response of imager pixels: (a) good pixel, (b) standard hot pixel, (c) hot pixel with offset.

The imager is generally referred to as a digital system, but the main pixel sensor is an analog device. The classic assumed response of any pixel to illumination can be modeled using Equation (1), where I_{pix} is the response, R_{photo} is the incident illumination rate, R_{dark} is the dark current rate, T_e is of the exposure time, b is the dark offset, and m is the amplification from the ISO setting.

$$I_{pix}(R_{photo}, R_{dark}, T_e, b) = m*(R_{photo}\ T_e + R_{dark}\ T_e + b) \tag{1}$$

For a good pixel, both R_{dark} and b are zero, resulting in the output response being a direct measure of the incident illumination. However, for a hot pixel, these two terms create a signal that is added onto the incident illumination, and therefore the pixel output appears to be brighter. The classical dark frame hot pixel offset model is shown in Equation (2).

$$I_{offset}(R_{dark}, T_e, b) = m*(R_{dark}T_e + b) \tag{2}$$

The dark response in Equation (2), sometimes called the combined dark offset, is linear. The parameters R_{dark} and b can be extracted by fitting a linear curve to the pixel dark frame response vs. the exposure time, as seen in Figure 1. For standard hot pixels, b is zero. These hot pixels are most visible in longer exposures as they do not have an initial offset. In the partially stuck hot pixel case, the magnitude of b affects the response and this defect will appear in all images. Obtaining this data for each camera involves typically 5 to 20 calibration images per test at a wide range of exposure times and ISOs, and their analysis with specialized software [2-4].

Using 29 DSLR cameras including both APS and CCD sensors and ranging from 1 to 11 years in age [9], we have been able to identify 243 hot pixels, of which 44% were of the partially stuck type at ISO 400. Partially stuck hot pixels have a greater impact on images than standard hot pixels as they are evident even at shorter exposures. The ISO setting in an imager controls the amplification or sensitivity of the pixel output. Higher ISO settings enable objects to be captured under low light conditions or with very short exposures. This removes the need for flash or a long exposure time when doing natural light photography. About 12 years ago, most DSLRs had ISO capabilities of 100 – 1600. As sensor technology improved and better noise reduction algorithms were developed, noise levels have been reduced and the usable ISO range has increased considerably, with recent DSLRs having an ISO range of 50 to 12,300 and high-end cameras having a range from 25,600 to 409,600 ISO.

Figure 2 shows the dark response of a hot pixel that we have measured for varying ISO levels. For low ISO, defects have low values of R_{dark} and b. Both R_{dark} and b increase dramatically, as the ISO amplification increases, scaling linearly with the ISO (see Equation (1)). In fact, at ISO 12800 the dynamic range of the pixel is

reduced by 40% solely due to the offset b, and at ISO 25600 the pixel is near saturation at all exposures. The high number of hot pixels with offsets suggests that the development of stuck-high pixels in the field may actually be due to the presence of hot pixels with very high offsets. This is consistent with our experience of not having detected a true stuck-high pixel in any of our cameras, while explaining the cameras developing stuck pixels discussed in camera forums.
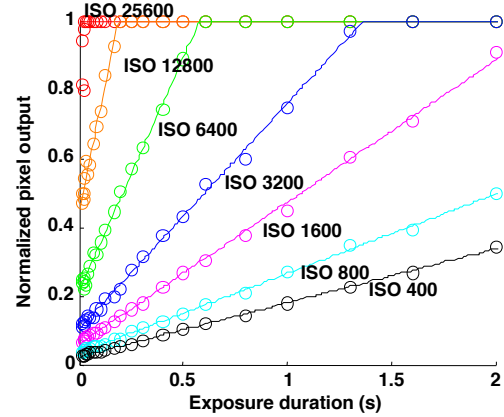

Figure 2: Dark response of a hot pixel at various ISO levels

Defect Growth Rate

In previous publications we have shown that hot pixel defects occurrences are randomly spaced across the imager [1-6], indicating that they are created by a random source such as cosmic rays. Other authors have reached a similar conclusion, and have argued that neutrons seem to create the same hot pixel defect types [7,8]. We recently developed, in [9], an empirical formula to relate the defect density D (defects per year per mm^2 of sensor area) to the pixel size S (in microns) and sensor gain (ISO) via the following equations:

For APS pixels:

$$D = 10^{-1.13}\ S^{-3.05} ISO^{0.505} \tag{3}$$

For CCD sensors

$$D = 10^{-1.849}\ S^{-2.25} ISO^{0.687} \tag{4}$$

These equations indicate that the defect rate increases drastically when the pixel size falls below 2 microns (see Figure 3), and is projected to reach 12.5 defects/year/mm^2 at ISO 25,600 (which is already available on some high-end cameras). Given that the current trend is to reduce the size of pixels, our experimental results project that the number of these defects will increase to high levels, emphasizing the need to understand how the development rate of these defects increases for even smaller pixel sizes.
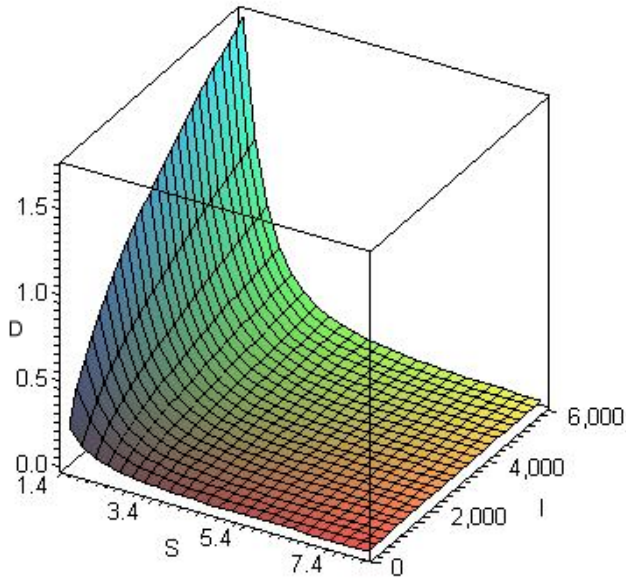
Figure 4: Camera count as a function of pixel size and ISO

Figure 3: Fitted power law for APS defect density (D=defects/year/mm^2) vs. pixel size S (µm) and ISO (I)

Defect Rates in Imagers with Smaller Sensors

The number of pixels in an average commercial digital camera has increased considerably in the last 11 years. In most cameras, the size of the sensor has remained the same but the size of the pixel has been reduced significantly, thus increasing the number of pixels on the sensor. In this study we have analyzed cameras ranging from DSLR cameras in the higher range pixel sizes (6 - 7 µm), point-and-shoot cameras in the midrange pixel sizes (3 - 4 µm) and cell phone cameras in the small pixel size range (2 - 3 µm). Figure 4 displays a 3D surface chart summarizing the range of imagers used and data collected in our previous research. On one axis, different pixel sizes are displayed. On the other, the different ISOs are presented. The vertical axis specifies the number of cameras used at a given ISO and pixel size.

Figure 4 shows that the previous research used imagers in the larger pixel size range and lower ISO ranges. One reason being that the majority of the imagers at the time had larger pixel sizes and smaller pixel technology had not made it into mainstream devices. An updated bar plot with our current data is displayed in Figure 5.

When comparing Figures 4 and 5 it is clear that our current research is expanding into the lower pixel sizes and a larger range of ISOs. Specifically at the 4 micron range, we have a large increase in the data set for ISO ranges. Even at the sub 2 micron range the ISO range has been enhanced. Additionally, it is important to note that each count on the above bar plot represents a large set of data for that pixel size and ISO combination. For each given pixel size and ISO combination we have about 10 data sets (images) ranging from 0.008 sec to 2 sec. For each hot pixel we conduct a linear regression fit for varying exposure times as shown in Figure 2. Furthermore, each imager contains calibration experiments over multiple times, giving us larger sets of data. Our oldest camera has undergone dark frame experiments at 15 different time points over 9.5 years, and most have 2 to 5 such periodic measurements. One should also note that Figure 5 displays a current snapshot and the smaller pixel range will be greatly enhanced in the near future as more imagers become available in this range. In past research we had collected data for both APS and CCD cameras. However, given that CCD sensors are only used in some scientific imagers and have ceased to be used in modern camera manufacturing, our future research will not continue to explore defects in CCD imagers and will concentrate on APS sensors only.
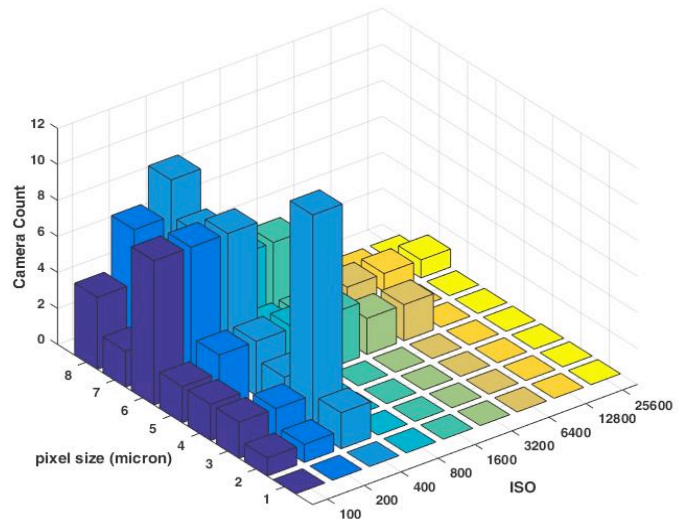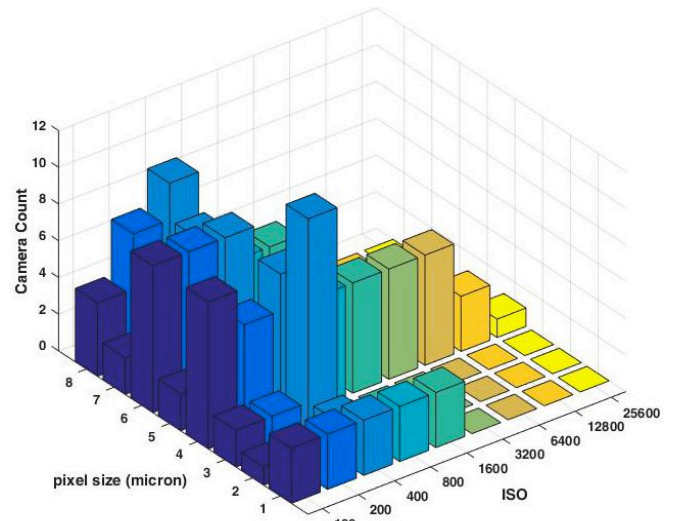

Figure 5: Updated camera count as a function of pixel size and ISO

In the original fitted curves shown in Equations (3) and (4), the data was concentrated at the 5 - 7 micron sizes for the full ISO range, while the smaller number of 3 - 4 micron pixels tended to have ISOs of 100-400. This caused the projections for small pixel sizes and higher ISO to have a higher uncertainty. The new data, shown in Figure 5, adds a significant number of points in the 1 - 4 micron pixel range with higher ISOs in the 1600-3200 range. This significantly reduces the uncertainty of the small pixel region of the curves.

For places where we only have a few data points for a given imager, we averaged the rate when doing the curve fitting. However, for imagers with a larger number of time points data sets (more than 2 tests), we did a linear regression for the rate fitting, to gain better statistical accuracy. Given that imagers are trending towards smaller pixel sizes, we believe that this data will prove to be quite beneficial for imager designers and users.

Table 1 shows how many sensors of a given area were tested and the types of cameras with those sensors. In terms of sensor area the DSLRS are mostly in the 330 to 350 mm^2 areas, with two at 850 mm^2 (full frame) size. Cell phone cameras ranged from 15 to 22 mm^2.

Table 1: Imaging sensor area for camera numbers tested

Area (mm^2)	Cameras	Type
16	3	Cell Phone
23	10	Cell Phone
340	18	DSLR
860	2	DSLR

Defect Analysis in Cell Phone Cameras

One area that we have been focusing our efforts on is the detection and analysis of hot pixels in cell phone imagers. This area of research has not been greatly explored in previous publications and is of growing interest as the application of cell phone cameras increases. This work is important as it reveals how hot pixels generation accelerates as pixel sizes decrease. As manufacturers push cellphone pixel sizes down to 1 micron, our goal is to provide a more accurate estimate of the hot pixel growth rate. Additionally, given the decreasing cost for cell phone manufacturing, manufacturers do not map out defects at the time of manufacturing, causing higher numbers of imager defects in cell phones compared to DSLR cameras where manufacturing defects are being mapped out.

In our earlier cell phone tests we used 10 identical phones of 2.2 micron pixel sizes. However, these phones had very limited exposure controls and would only output images in JPEG format. While we did develop techniques to detect hot pixels, the compressed image format made extraction of the pixel parameters quite difficult and gave low precision [10].

This area of research requires different experimental methods in terms of image extraction, detection, and analysis, in contrast to what is typically used in experiments with DSLRs. First, the extraction of true digital RAW images from cell phone imagers is quite difficult. Extraction of RAW images is not supported with iOS cell phones. Some variants of Android do support RAW, but only on specific cell phone models and OS versions (5.1 and greater) where the manufacturers have fully implemented the RAW support set. Another complication is that these RAW images are quite noisy in nature, making the identification and analysis of hot pixels a non-trivial task. As cell phones sensors heat rapidly, we need to separate each exposure (image) by 30 sec or the phone heating changes will dominate. Furthermore, it turns out to be best to fully turn off the phone and let it cool to room temperature before turning it on for any test set. This is due to the inherent lack of noise suppression algorithms in cell phone imagers as compared to those used in DSLR cameras. To handle this, we have developed specialized detection algorithms that enable us to obtain a defect count for various cell phone imagers. We also ensure that hot pixel detections in cell phone cameras are statistically significant within the error margins. If either the fitted offset or dark current is statistically significant, the hot pixel will be regarded as a true hot pixel. If neither is significant, then it will be considered as noise.

Initial results suggest that the number of hot pixels that occur in RAW images from most cellphone imagers is very high (ranging between 100 and 500 hot pixel defects). It turns out that most cell phone manufacturers do not map out the fabrication time defects as they do in DSLRs. This requires that we get sufficient measurements over time to do a linear regression back to time zero to identify those initial fabrication time defects. Fortunately (for analysis purposes only), as defect numbers in small pixels increase rapidly over time (e.g., 5 in a month at ISO 400 for 1.8 micron pixels), this can be done with a modest set of measurements over a few months. In the near future, more cellphones will switch to newer OS versions that support RAW image formats, which will in turn increase our range of cellphone cameras available for defect analysis. Currently, as Figure 5 demonstrates, we are able to test cell phone cameras with pixels from 1.5 to 1.1 microns, and ISOs from 400 to 1600 ISO. The highest ISOs

that each cell imager permits were always found to be too noisy to extract data from.

These small (e.g., 1.1 micron) pixel results showed defect/year/mm^2 rates that ranged up to 100 times higher than those of DSLRs with 4 micron pixels. This is in line with the power law type relationship of defect density to pixel size that we noted in our earlier research.

Small Pixel Fitted Results

Using the new data sets for the APS sensors, we concluded that the defect rate curve has changed only slightly from the previous one in Equation (3) to

$$D=10^{-1.12}S^{-3.15}ISO^{0.522} \qquad (5)$$

The modest changes compared to Equation (3) imply that the predicted trends still hold. More importantly, the standard errors of the new fitted values are smaller. Pearson's r correlation coefficient for this fit is r=0.91, which indicates a strong fit and small average errors. The fitted power of the pixel size S, when taking into account the standard error, is 3.15 ±0.17, a range that includes the original power in Equation (3). As Figure 6 shows, this indicates that the defect rate increases by 8.9 times as pixels shrink by a factor of 2, say from 4 microns (current DSLR range) to 2 microns (where cell phones start now). Defect rates also increase with ISO to the power of 0.522±0.08 which means that going from ISO 400 to 3200 (a common range now) results in a 3 times increase in the defect rate.
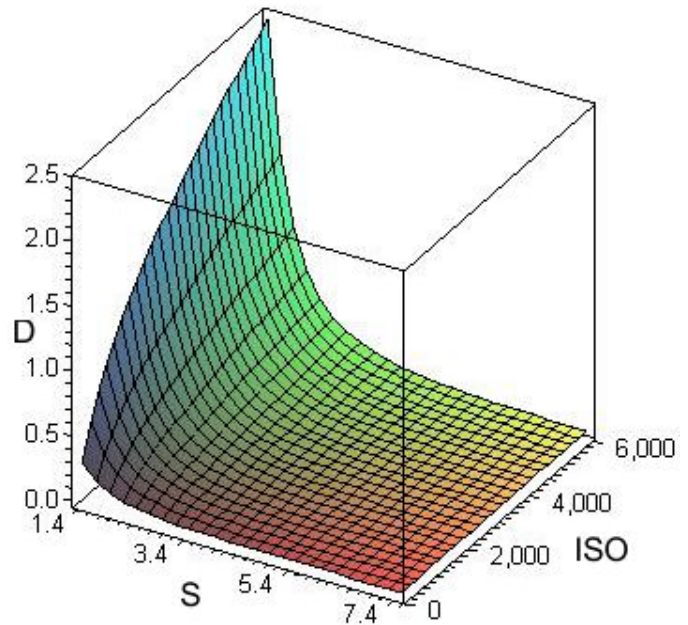

Figure 6: Expanded data Fitted power law for APS defect density (D=defects/year/mm^2) vs. pixel size S (µm) and ISO (I)

Of great importance are the defect rates in the cell phone current range, which is from 2.5 micron to the 1 micron pixels that manufacturers are aiming at. Moreover, cell phones are now targeting ISOs of 3200 to 6400 in order to approach the dark scene capability of DSLRs. Figure 7 shows how the defect rates will accelerate as 1 micron pixels are approached. Note that the vertical defect rate scale is now increased by a factor of 2.6.
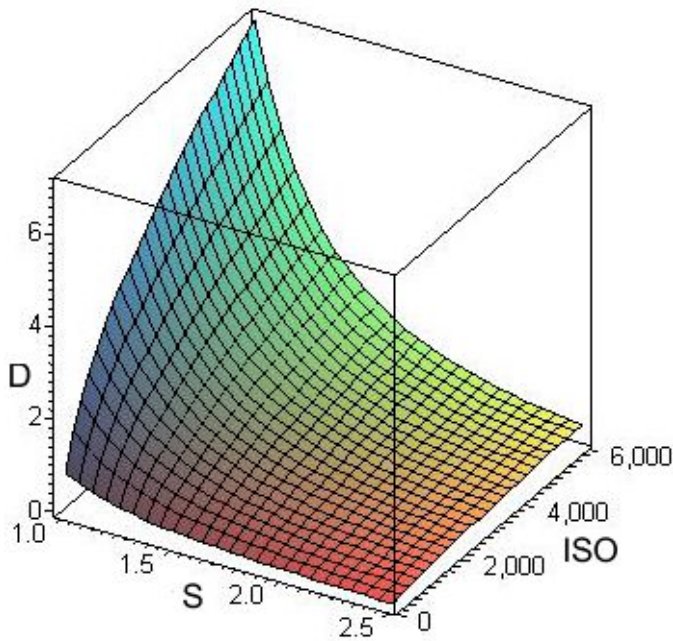
Figure 7: Expanded data Fitted power law for APS in the 1 to 2.5 µm pixel range: defect density (D=defects/year/mm^2) vs. pixel size S (µm) and ISO (I)

Figure 9: Residuals of fitted power law for APS defect density; Residual Log(D) (D=defects/year/mm^2) vs. pixel size S (µm)

Figure 10: Residuals of fitted power law for APS defect density; Residual Log(D) (D=defects/year/mm^2) vs. ISO

An important measure of any fit is the distribution of the residual errors (difference between the fitted and actual data). As this is a power law relationship we plot the residuals of Log(D) against the pixel size S and ISO. For better analysis we observe the residuals against the pixel size S in Figure 9, and against the ISO in Figure10. Note that the residuals are quite evenly distributed on both sides of the zero axis for both plots, indicating no systematic deviations with ISO or pixel size S. The residuals at 2.2 microns are clustered on the positive side, but these are all from earlier cell phone tests which only had access to the jpeg images. These tests have more difficulty in detecting hot pixels, and limited camera control compared to the RAW images used for the other data points. It is noted that the largest deviations are for the high ISO1600 and ISO3200 ranges. This is understandable as these are the noisiest operating regions of even the DSLR cameras.
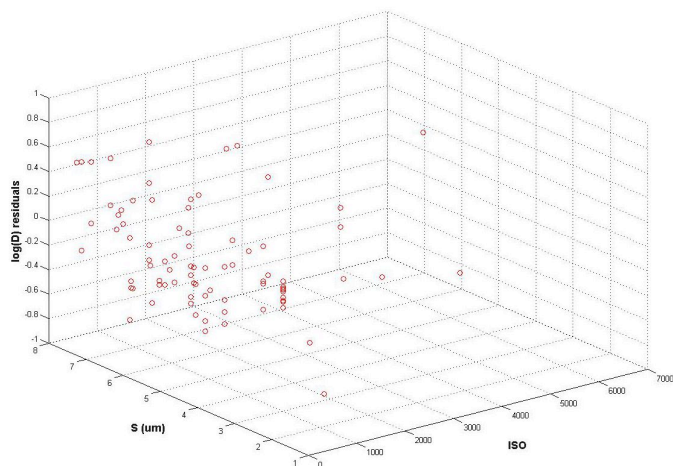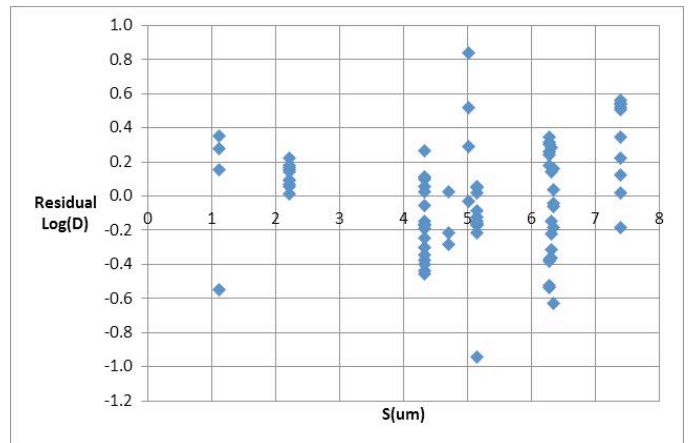

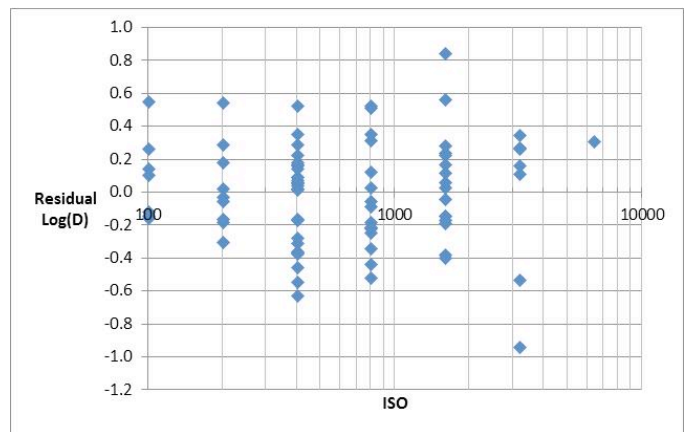Figure 8: Residuals of fitted power law for APS defect density; Residual Log(D) (D=defects/year/mm^2) vs. pixel size S (µm) and ISO

Our most recent measurements on the smaller 1.4 to 1.1 m pixels with higher ISO ranges are in alignment with our previous projections for the rapid growth of defect rate as pixels approach the one micron size. As a matter of fact, based on our very recent cell phone measurements, we believe that these curves are a conservative estimate of the actual defect rate. The fit errors are largest in the smaller pixel sizes, due to the lower number of data points. At the 1.1 micron pixels we are seeing rates of 5.8 defects/year/mm^2 at 1600 ISO.

Since the newest generation of cell phones have the digital raw imaging implemented in the OS, we expect to significantly expand both the number and accuracy of these data points in the next few months.

This conclusion has important implications for imager designers as they push down to the one micron or smaller pixels. This is further exacerbated by moving ISOs closer to the 6400 or 12,800 values common in DSLRs. The strong indication is that defect numbers will become significant even at these small sensor areas (15-25 mm^2) and even with the few years lifetime of typical cell phone ownership. For DSLR designers, were sensor sizes are typically more than 10 times larger, moving the pixel sizes towards 2 microns will significantly increase their defect rates even with the lower noise sensors available for those cameras. Moreover, the much longer ownership lifetime of those DSLRS, combined with a greater sensitivity of the users to defects, makes this potentially a larger issue for them.

With imaging sensors moving into many other products, like car cameras, which have even longer lifetimes (with design targets of up to 20 years of in field usage), this can have other reliability issues. For example, when these cameras are being used as part of driving automation, where edge detection algorithms are important, hot pixels growth over long periods of time can have a significant impact.

Conclusions

This paper emphasizes the strong defect growth behavior of hot pixels as pixels sizes are shrunk, especially to the 2 to 1 micron range. Our current results show a significant accelerated defect growth rate in this small pixel range due to the power law relationship with pixel size. The current fit suggests that a shrinkage of the pixel size by a factor of 2 results in an 8.9 times increase in the defect rate. The growth with higher imager sensitivities (ISOs) only increases this effect, with a factor of 2 increase in ISO generating a 1.44 increase in defect rates. Such increases are of significant importance for DSLRs where serious and professional photographers are very sensitive to significant numbers of defects in their images.

Cell phone cameras, which are the best source of 2-1 micron pixels for testing, have just implemented digital raw formats in the past year. Our tests showed that using this format was needed for accurate measurements of hot pixels. Growing numbers of cell phones using this format by the end of 2015 will give us much larger data sets in these small pixel sizes in the near future. The defect rate equations we obtained suggest care in the current race for even smaller pixels (thus more megapixels) in cell phones. Even for these small area sensors, shrinkage below 1 microns is projected to produce defect rates that may degrade the image even for the short lifetime ownership of current phones (1 to 2 years).

With these clear results, imager designers need to take this strong relationship between pixel size and defect rates into account during system planning.

References

[1]   J. Dudas, L.M. Wu, C. Jung, G.H. Chapman, Z. Koren, and I. Koren, "Identification of in-field defect development in digital image sensors," *Proc. Electronic Imaging, Digital Photography III*, v6502, 65020Y1-0Y12, San Jose, Jan 2007.

[2]   J. Leung, G.H. Chapman, I. Koren, and Z. Koren, "Statistical Identification and Analysis of Defect Development in Digital Imagers," *Proc. SPIE Electronic Imaging, Digital Photography V*, v7250, 742903-1 – 03-12, San Jose, Jan 2009.

[3]   J. Leung, G. Chapman, I. Koren, and Z. Koren, "Automatic Detection of In-field Defect Growth in Image Sensors," *Proc. of the 2008 IEEE Intern. Symposium on Defect and Fault Tolerance in VLSI Systems*, 220-228, Boston, MA, Oct. 2008.

[4]   J. Leung, G. H. Chapman, I. Koren, Z. Koren, "Tradeoffs in imager design with respect to pixel defect rates," *Proc. of the 2010 Intern. Symposium on Defect and Fault Tolerance in VLSI*, 231-239., Kyoto, Japan, Oct 2010.

[5]   J. Leung, J. Dudas, G. H. Chapman, I. Koren, Z. Koren, "Quantitative Analysis of In-Field Defects in Image Sensor Arrays," *Proc. 2007 Intern. Sym on Defect and Fault Tolerance in VLSI*, 526-534, Rome, Italy, Sept 2007.

[6]   J. Leung, G.H. Chapman, Y.H. Choi, R. Thomson, I. Koren, and Z. Koren, "Tradeoffs in imager design parameters for sensor reliability," Proc*., Electronic Imaging, Sensors, Cameras, and Systems for Industrial/Scientific Applications XI*, v 7875, 78750I1-0I12, San Jose, Jan. 2011.

[7]   A.J.P. Theuwissen, "Influence of terrestrial cosmic rays on the reliability of CCD image sensors. Part 1: experiments at room temperature," *IEEE Transactions on Electron Devices*, Vol. 54 (12), 3260-6, 2007.

[8]   A.J.P. Theuwissen, "Influence of terrestrial cosmic rays on the reliability of CCD image sensors. Part 2: experiments at elevated temperature," *IEEE Transactions on Electron Devices*, Vol. 55 (9), 2324-8, 2008.

[9]   G.H. Chapman, R. Thomas, I. Koren, and Z. Koren, "Empirical formula for rates of hot pixel defects based on pixel size, sensor area and ISO", *Proc. Electronic Imaging, Sensors, Cameras, and Systems for Industrial/Scientific Applications XIII*, v8659, 86590C-1-C-11 San Francisco, Jan. 2013.

[10] J. Leung, "Measurement and Analysis of Defect Development in Digital Imagers, MASc thesis, Simon Fraser University, School of Engineering Science, Burnaby, BC Canada, 2011.

Author Biographies

Glenn Chapman, Professor, School of Engineering Science, Simon Fraser University, Canada, researching in defects in digital image sensors. BSc and MSc Physics Queen's University, and PhD McMaster University, Canada.

Israel Koren, Professor, Electrical and Computer Engineering at the University of Massachusetts, Amherst and a fellow of the IEEE. BSc, MSc and DSc Technion - Israel Institute of Technology.

Zahava Koren, senior researcher, University of Massachusetts, Amherst. B.A and M.A degrees in Mathematics and Statistics, Hebrew University, Jerusalem, and D.Sc. degree Operations Research, Technion - Israel Institute of Technology.